Elsevier Editorial System(tm) for Planetary and Space Science
Manuscript Draft

Manuscript Number:

Title: Properties of plasma near the Moon in the magnetotail

Article Type: SI:solar wind planet interac

Keywords: Moon; Magnetotail; Solar wind; Plasma-surface interaction; MHD simulation; Debye layer

Corresponding Author: Dr. Esa Kallio,

Corresponding Author's Institution: Finnish Meteorological Institute

First Author: Esa Kallio

Order of Authors: Esa Kallio

Abstract: Plasma physical processes near the lunar surface depend on the properties of the ambient plasma. However, the Moon spends almost half of its time downstream of the Earth's bow shock where the plasma near the Moon is anticipated to differ from the undisturbed solar wind. We have made statistical analysis of plasma parameters and the magnetic field near the orbit of Moon by using a global magnetohydrodynamic simulation made for a time period which covers a full year. The study shows that the velocity and the magnetic field downstream of the bow shock near the lunar orbit are much alike in the solar wind. This suggests that these plasma parameters near the Moon is controlled and driven by the solar wind. Density and temperature of the plasma are, however, strongly modified by the Earth. Consequently, the characteristic length scale of the plasma layer above the lunar surface, the Debye length, is controlled by plasma physical processes in the Earth's magnetosphere. The derived plasma and field parameters make it possible to analyse in detail the direct plasma-surface interaction at the Moon when it is in the magnetotail.

Highlights

- Statistical analysis of plasma parameters and the magnetic field near the orbit of Moon has been made

- Data set is based on a MHD simulation for the time period Jan 2002 – Feb 2003

- Derived parameters make it possible to analyse in detail the direct plasma-surface interaction at the Moon when it is in the magnetotail

Figure_1

FIGURE 1

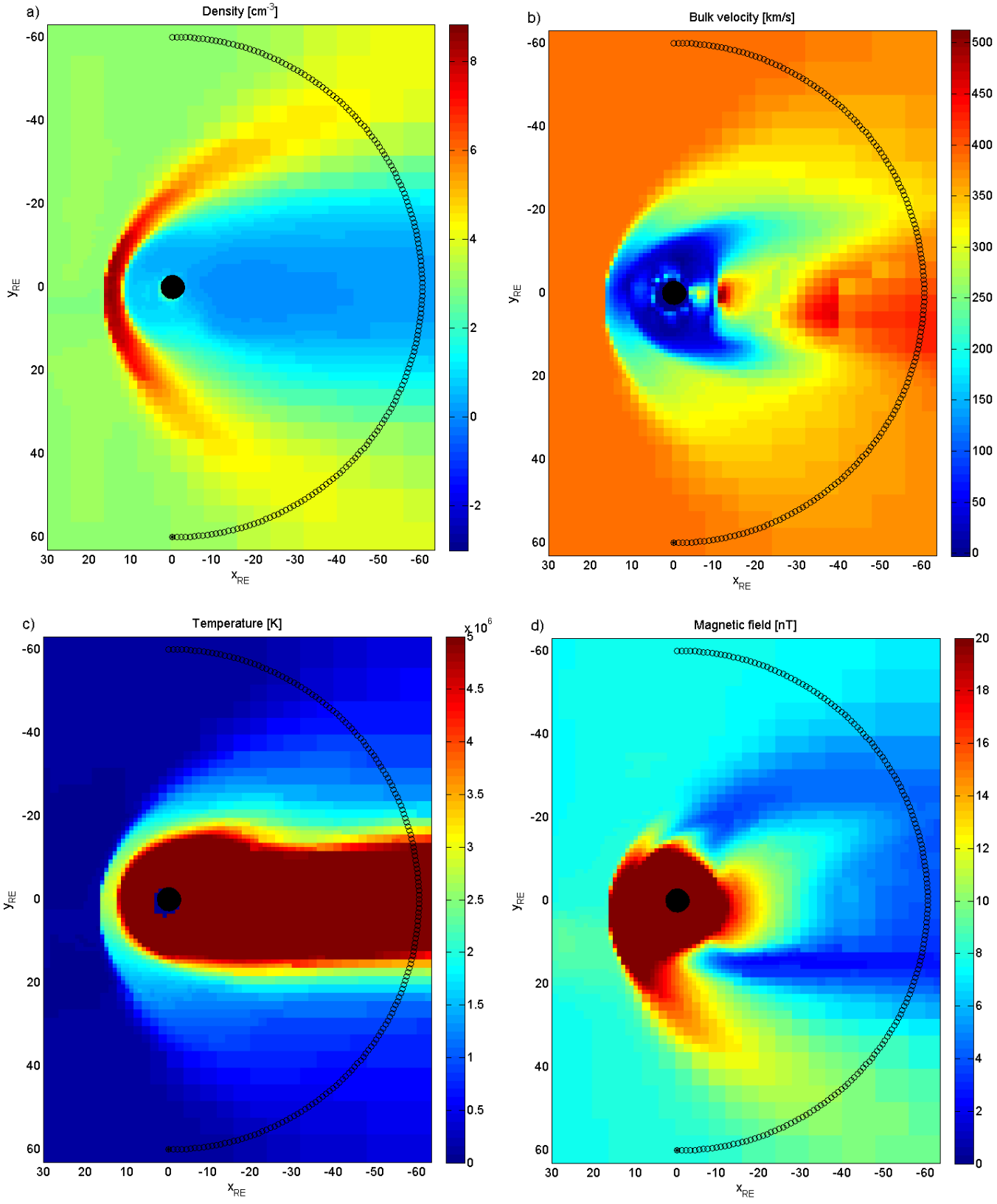

Figure_2

FIGURE 2

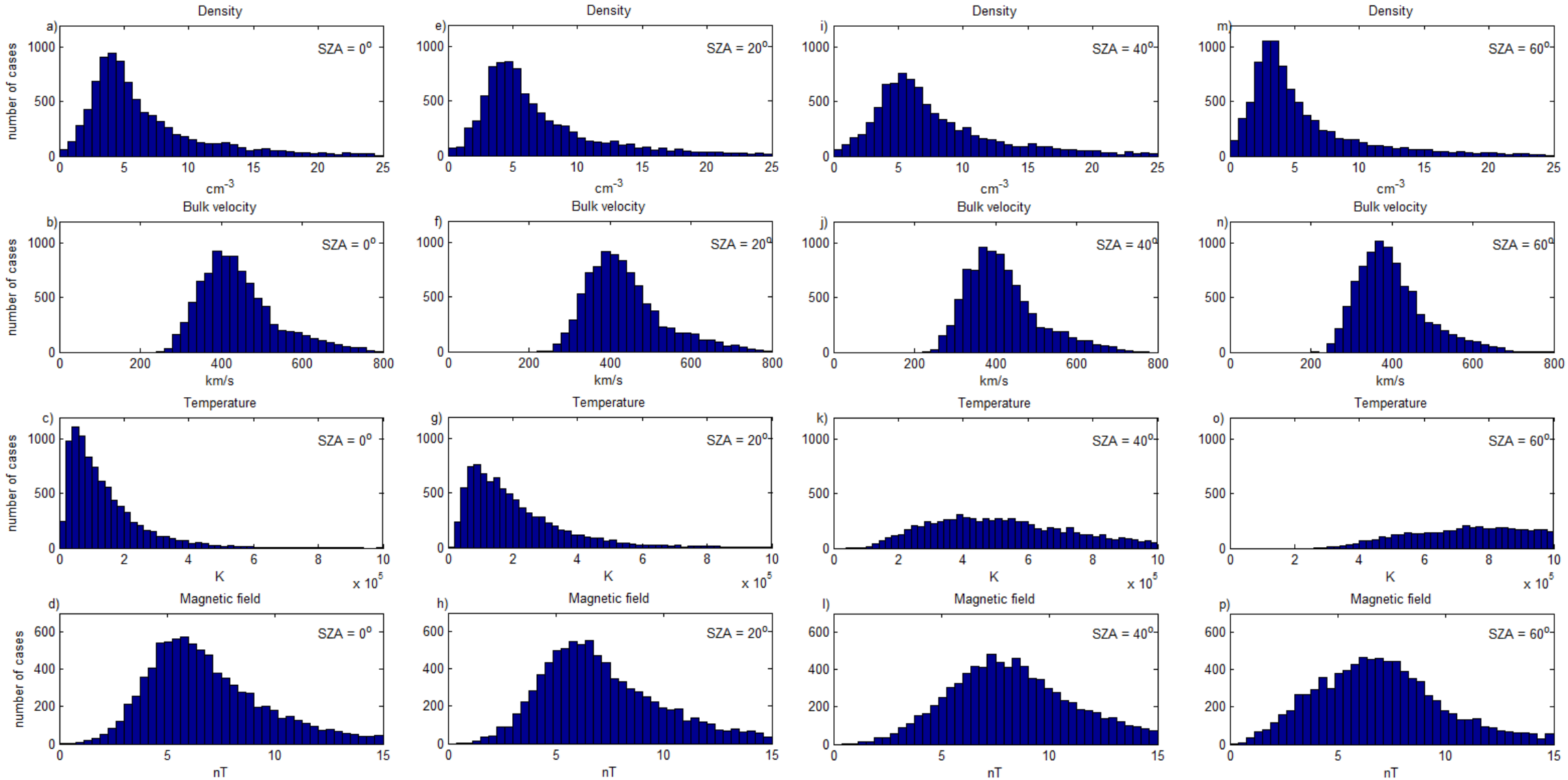

Figure_3

FIGURE 3

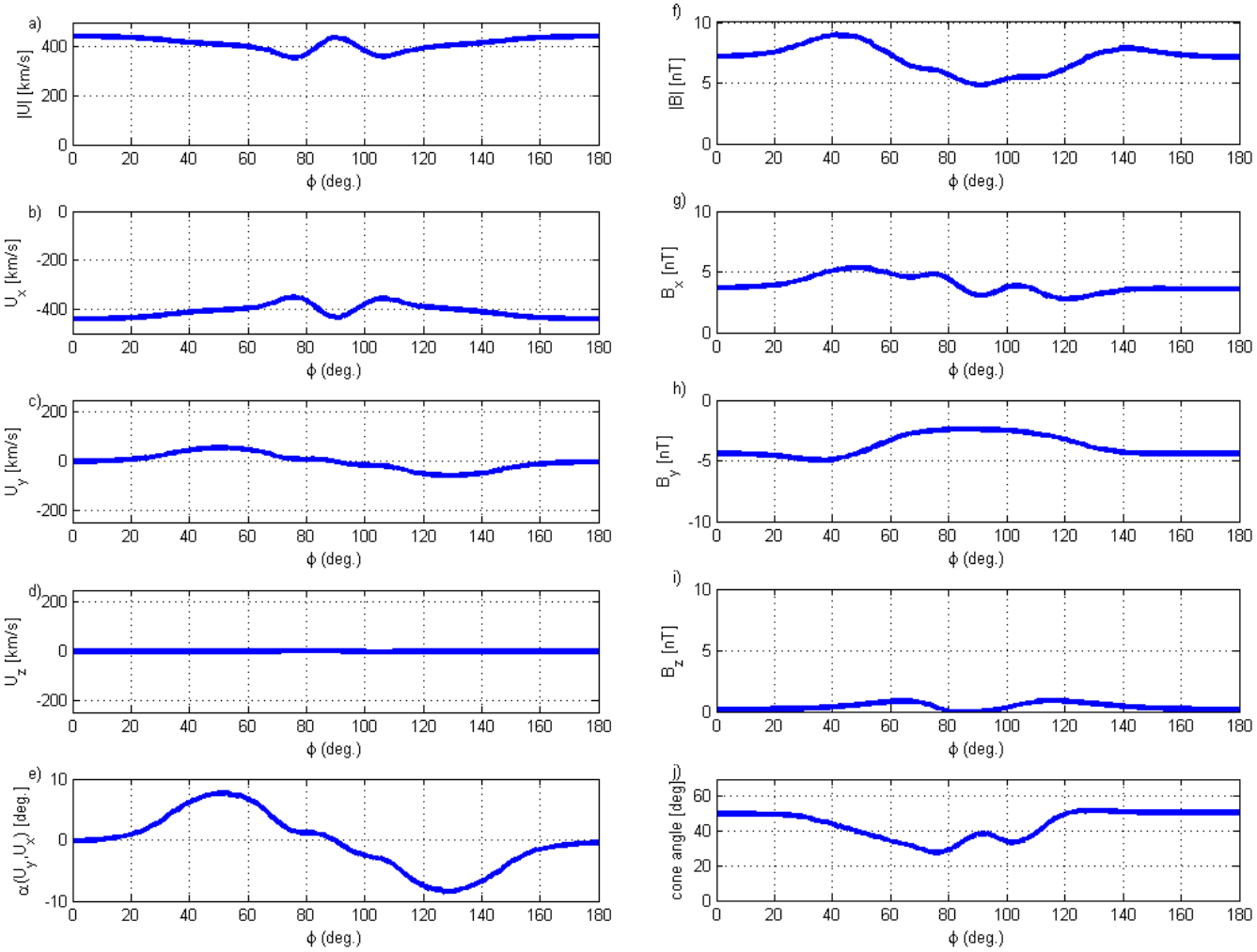

Figure_4

FIGURE 4

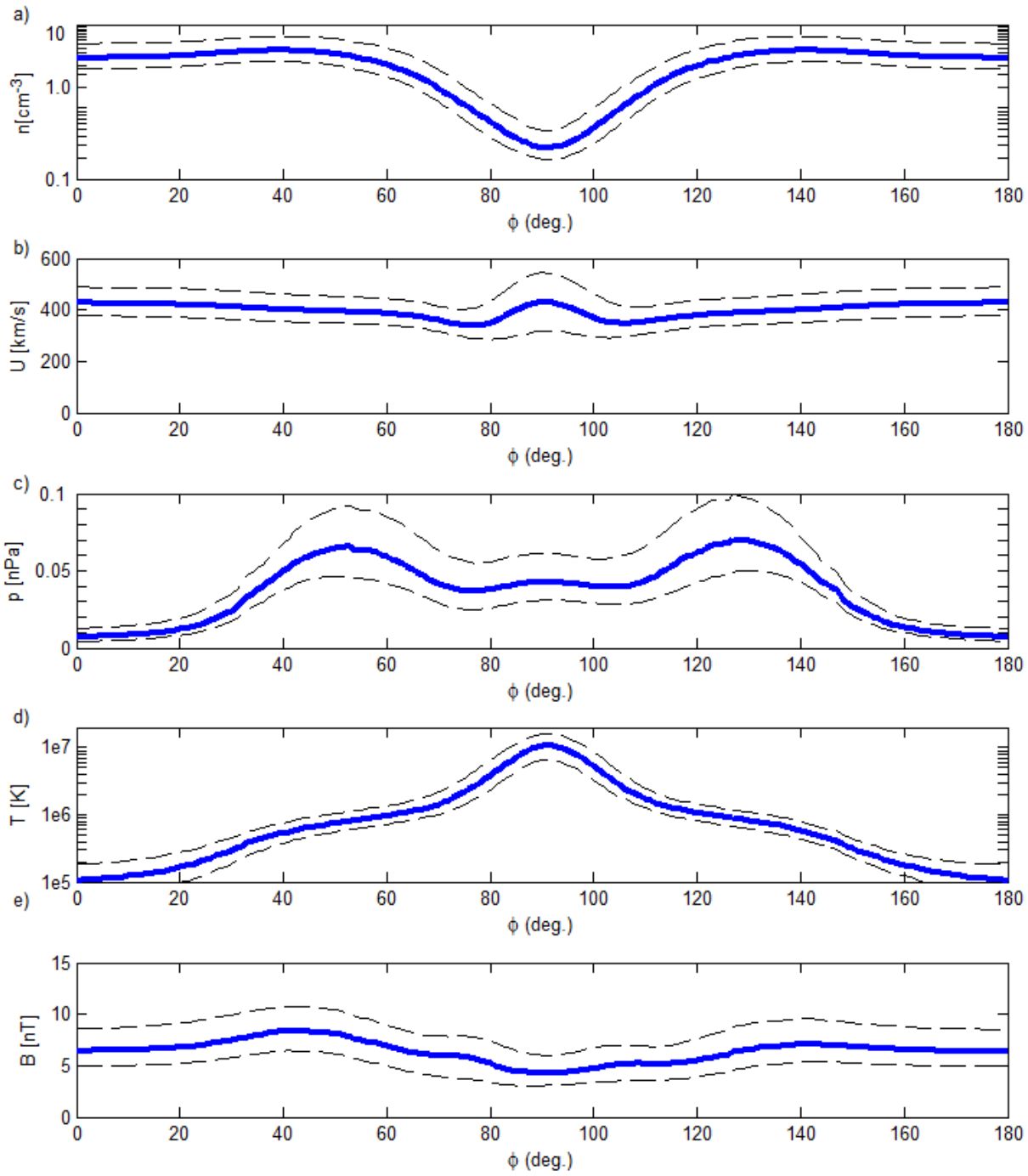

Figure_5

FIGURE 5

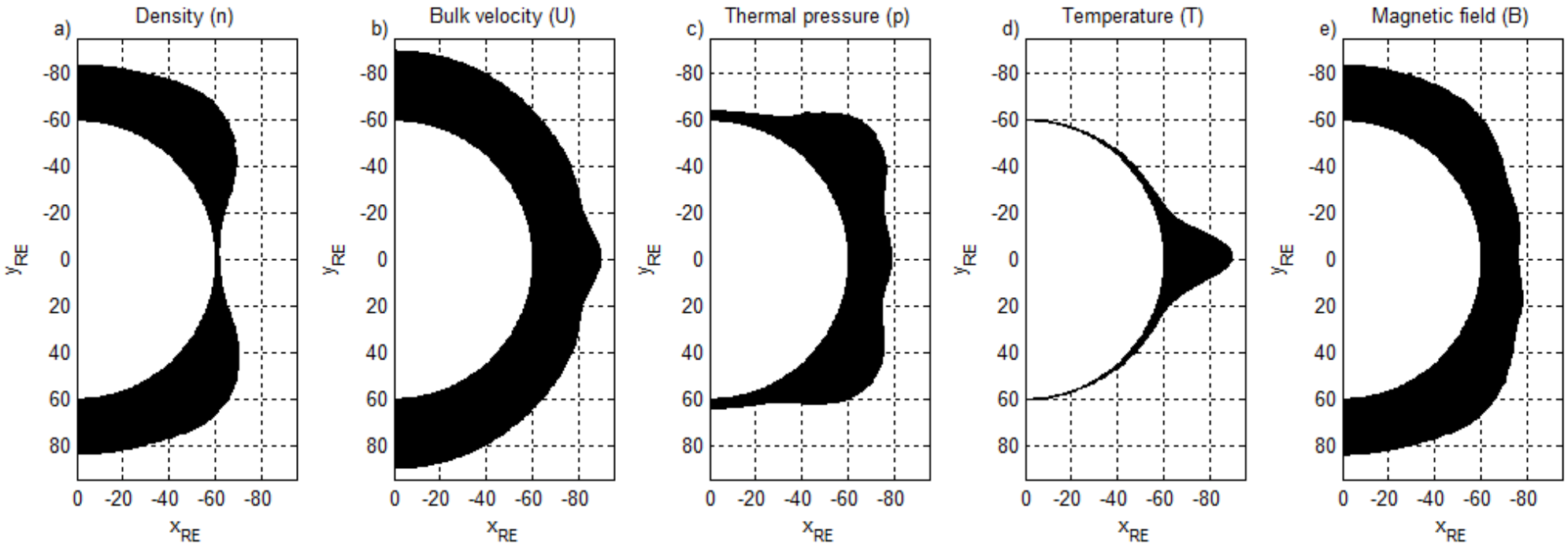

Figure_6

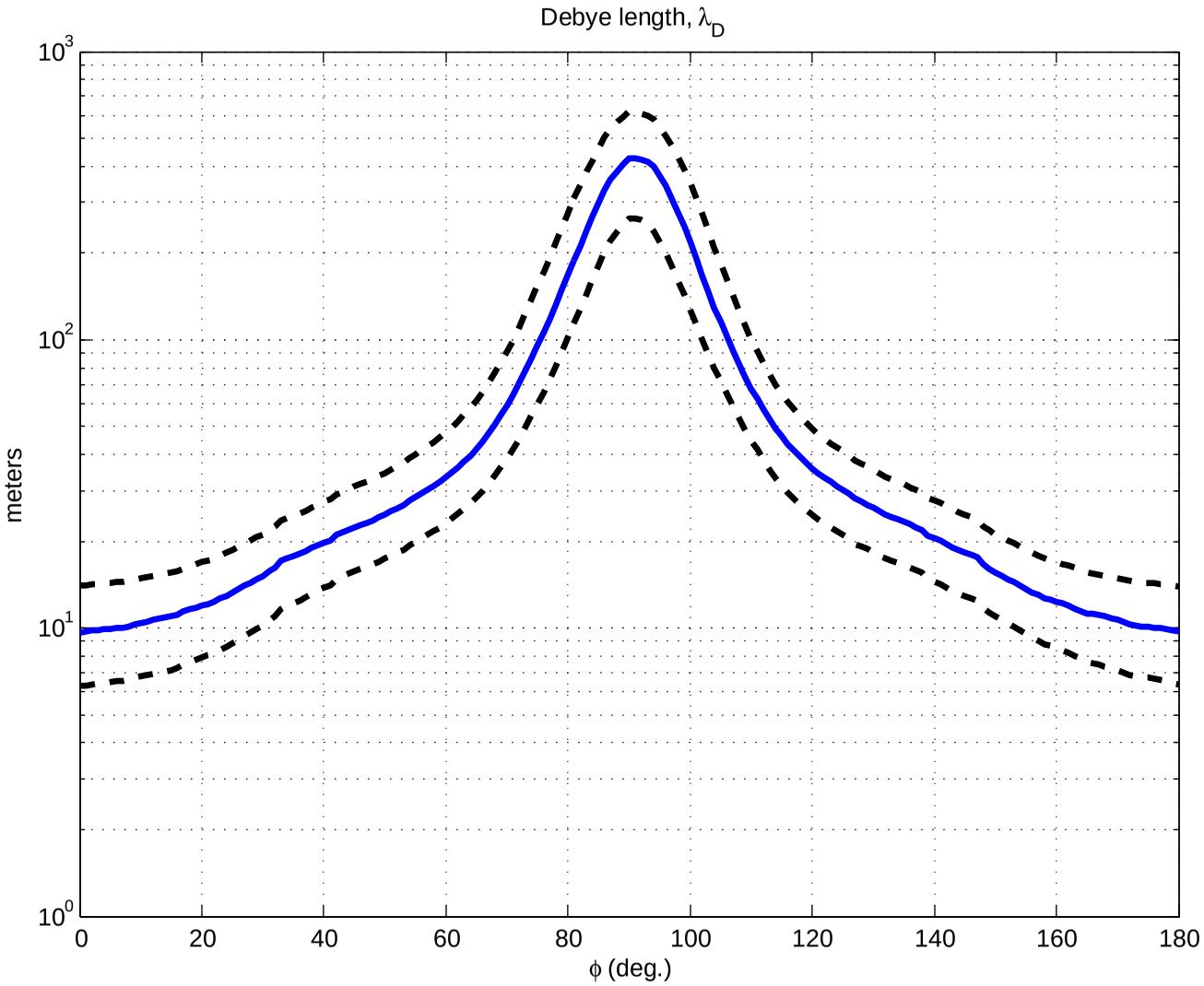
Debye length, λ_D
10^3
10^2
10^1
10^0
meters
0
20
40
60
80
100
120
140
160
180
ϕ (deg.)

Properties of plasma near the Moon in the magnetotail

Esa Kallio[1,2] and Gábor Facskó[3]

1: Aalto University, School of Electrical Engineering, Helsinki, Finland (esa.kallio@aalto.fi)

2: Finnish Meteorological Institute, Helsinki, Finland

3: Geodetic and Geophysical Institute, Research Centre for Astronomy and Earth Sciences, Hungarian Academy of Sciences, Sopron, Hungary (facsko.gabor@csfk.mta.hu)

Abstract

Plasma physical processes near the lunar surface depend on the properties of the ambient plasma. However, the Moon spends almost half of its time downstream of the Earth's bow shock where the plasma near the Moon is anticipated to differ from the undisturbed solar wind. We have made statistical analysis of plasma parameters and the magnetic field near the orbit of Moon by using a global magnetohydrodynamic simulation made for a time period which covers a full year. The study shows that the velocity and the magnetic field downstream of the bow shock near the lunar orbit are much alike in the solar wind. This suggests that these plasma parameters near the Moon is controlled and driven by the solar wind. Density and temperature of the plasma are, however, strongly modified by the Earth. Consequently, the characteristic length scale of the plasma layer above the lunar surface, the Debye length, is controlled by plasma physical processes in the Earth's magnetosphere. The derived plasma and field parameters make it possible to analyse in detail the direct plasma-surface interaction at the Moon when it is in the magnetotail.

1. Introduction

Plasma physical processes near the Moon depend on the properties of the ambient plasma. The Moon does not have an atmosphere or a global intrinsic magnetic field and, therefore, the plasma can interact directly with the surface. This interaction results in physical processes at wide length scales of order of meters to the size of the Moon.

The direct plasma-surface interaction results in small scale physical processes near the lunar surface within a sheath region, the Debye layer, where an electric field is formed due to the charge separation between solar wind protons and electrons from the solar wind and photoelectron from the lunar surface. The size of the Debye layer and the electric field within it depend on the properties of the ambient solar wind plasma, properties of the surface and the strength of the solar EUV light. The Debye layer in turn affects the properties of dust particles from the Moon because the electric field accelerates charged dust particles above the surface (see e.g. Nitter et al., 1998).

Large scale plasma physical processes associated with the direct plasma-surface interaction are the formation of a tail region behind of the Moon and escape of ions of a lunar origin which are picked up by the flowing plasma. The properties of the tail, such as the length of the tail and plasma within it, are controlled by the plasma, the electric and the magnetic fields (e.g. Kallio 2005; Holmström et al., 2012). Moreover, the Lorentz force depends on the electric and magnetic fields and, therefore, properties of pick-up ions are controlled by the properties of ambient plasma (e.g. Mall et al., 1998).

The length scale of the Debye layer in a nominal solar wind conditions is an order of a meter while the length size of the tail and the gyroradius of the heave pick-up ions are order of the radius of the Moon (~1740 km). Interesting physical processes also takes in place around lunar magnetic anomalies in a length scale between the "global scale" and "micro scale". In those "meso scale" processes the localised magnetic field is strong enough to affects the motion of the solar wind plasma and the properties of plasma within the Debye layer (see Kallio et al., 2012, for further discussions about physical processes at different length scales).

Detailed analysis of aforementioned plasma physical processes requires therefore knowledge of the properties of the plasma near the Moon. In 3D plasma models the properties of plasma and field in the lunar tail has been studied by 3D hybrid models (Kallio 2005; Holmström et al., 2012). Recently physics within the Debye layer and the properties of lunar dust has analysed by local full kinetic models (e.g. Poppe and Horànyi, 2010; Kallio et al., 2014). Furthermore, lunar magnetic anomaly regions have been studied by tests particle simulations and hybrid models (e.g. Kallio et al. 2012; Jarvinen et al., 2014; Kallio et al., 2014).

A detailed analysis of the situation where the Moon is in the solar wind can be made when the Moon is in the solar wind by using observations from the satellite measurement near the Earth (e.g. the Wind satellite) and in the Lagrange point (the ACE satellite). However, the Moon spend almost half of its time downstream of the Earth's bow shock where the Earth has affected the properties of the solar wind plasma. One may therefore ask how much the properties of plasma in this disturbed region differ from the undisturbed solar wind? Furthermore, which of the plasma parameters differs mostly from the upstream parameters and at what places along the orbit of the Moon largest charges can be seen? Moreover, are statistical properties of the plasma near the Moon similar than statistical properties of the plasma in the solar wind or does the Earth change statistical properties by its magnetospheric processes?

The goal of this paper is to analyse properties of plasma near the lunar orbit by using a new data set derived from a 3D magnetohydrodynamic GUMICS-4 model. Recently, 3D magnetohydrodynamic models have been shown to provide new insight on the properties of plasma in the Earth's tail at lunar distances (Sibeck et al., 2014; Vörös et al., 2014). Statistical parameters were derived by using simulated plasma parameter for the time period Jan. 2002 – Feb. 2003. The power of the adopted approach is that in a 3D model we know always exact upstream parameters and, therefore, we can study the correlation and response of the plasma parameters on the orbit of the Moon simultaneously within the Earth's magnetosphere and in the solar wind. In such a way the role and contribution of the Earth can be studied statistically.

The paper is organized as follows. First, the used 3D MHD model and the generation of the data set are described. Then the data set is used to analyse the distribution of plasma parameters and the statistical properties of plasma parameters near the orbit of the Moon. Finally, pros and cons of the data set and the analysis are discussed.

2. The model and the data

2.1 Description of the model

The simulated data was obtained from Grand Unified Magnetosphere Ionosphere Coupling simulation (GUMICS, version 4) model developed at the Finnish Meteorological Institute. The size of the simulation box was +32 R_E to -224 R_E in the X direction and ±64 R_E in the Y and Z directions in Geocentric Solar Ecliptic (GSE) coordinates where the X-axis points from the centre of the Earth to the Sun, the +Z-axis points to the ecliptic North and the Y-axis completes the right hand coordinate system (R_E = 6378 km is the used radius for the Earth). The default size of the grid was 2 R_E which was adaptively refined during the run. In the tail the grid resolution was 2 R_E , 1 R_E, 0.5 R_E or 0.25 R_E depending on the position. Outflow conditions were applied at all

boundaries of the simulation box except at the sunward boundary, where the input was given to the simulation. The GUMICS-4 used two simulation domains: The ionospheric domain, which is a tilted dipole field region within 3.7 R_E, and the magnetospheric domain outside the ionospheric domain. These domains were coupled to each other, which was updated every four seconds in the simulation (see more in Janhunen et al., 2012, and references therein).

2.2 A year GUMICS simulation

One year global MHD simulation was made using 1 min resolution OMNIWeb solar wind plasma and the magnetic field data as inputs. The solar wind time series from February 1, 2002 to January 31, 2003 were selected because the total length of the data gap was the shortest in this 365 days long period. In practice, the simulated one year long interval was divided into short time periods simulations. In total 368 days (or 155 Cluster space craft orbits) were selected as input to the GUMICS-4 simulation. Each Cluster orbit was divided into 12 subintervals with an hour initialization time to accelerate the simulation. The IMF B_x magnetic field component was replaced by its mean value for all intervals. The average dipole tilt angle was set for each simulation intervals. The simulation results were typically saved in every 5 min (see Facskó et al., 2014, for technical details of the one year GUMICS-4 simulation).

2.3 Solar wind parameters along the Moon orbit

The Moon is inclined ~5° to the ecliptic elliptical orbit around the Earth and its orbit perturbed by the Sun, Venus and Jupiter mainly (see, e.g. SPICE toolkit at http://naif.jpl.nasa.gov/naif/toolkit.html for the details of the lunar orbit for a given time period). The average radial distance (r_M) of the Moon in the analysed case was ~60.2 R_E. The minimum and maximum r_M was 55.7 R_E and 63.5 R_E, respectively. The average z_{GSE} of the Moon was -0.3 R_E and the minimum and maximum z_{GSE} were -5.8 R_E and 5.4 R_E, respectively. Therefore, the orbit of the Moon was within the region of r_M ~ [55, 63] R_E and z_{GSE} ~ [-6, 6] R_E. In this paper the plasma parameters were derived near the average position of the Moon at positions on the half circle (x_{GSE}, y_{GSE}, z_{GSE}) = ($60R_E$ $\cos(90^o + \phi)$, $60R_E$ $\sin(90^o + \phi)$, 0) where $\phi = 0^o,1^o,..,180^o$ and R_E = 6378 km, that is, in total 181 positions. Note that one degree corresponds about 1 R_E resolution on the lunar orbit.

In this paper the particle density (n), the solar wind velocity components (U_x, U_y, U_z), the thermal pressure (p) and the magnetic field components (B_x, B_y, B_z) were derived from one saved simulation file per an hour along the half circle. The plasma temperature, T (≡ p/nk where k is the Boltzmann's constant) was derived from the thermal pressure and the plasma density. For each hour the closest saved file was selected. The parameters along the orbit were derived from the grid by using a linear interpolation. The total number of derived data points at every 181 positions was 8811 which corresponds the time interval of about 367 days. The formed data set was used in this paper to study statistical properties of the solar wind plasma and the magnetic field near the Moon.

3. Results

Before studying in detail the properties of the plasma parameters on the lunar orbit is important to put the data in a wider context and to analyse how the lunar orbit passes different plasma boundaries and region in the Earth's magnetotail.

Fig. 1 gives an example of solution obtained from the GUMICS-4 model at Feb 20, 2002, 08:54 UT where the density (n), the bulk velocity (U) and the temperature (T) of the solar wind and the total magnetic field (B) are shown on the GSE XY-plane. The undisturbed upstream parameters, determined at the point (30.5, −63.4, 0) R_E, were n ~ 3 cm^{-3}, U ~ 390 km/s, T ~ 85 000 K and **B** ~ [-5, 6, 0] nT. The terrestrial dipole tilt angle was −15.2° on the GSE XZ-plane. The parameters were derived without interpolation in order to illustrate the size

of the grid in the tail which was 0.25 − 2R_E. If we look how plasma parameters changes when ϕ increases from 0^o to 90^o we see how vantage point is first in the solar wind at (0, 60 R_E, 0) and then it crosses the bow shock and enters into the magnetosheath where the plasma density and pressure increases. The next plasma region is the magnetotail where the plasma density decreases and plasma pressure increases when the centre of the tail is approached. Within the magnetotail the properties of plasma depends on whether the analysed position is inside the magnetic tail lobes or inside the plasma sheet within the lobes.

In reality the solar wind parameters vary in time and, consequently, also the positions of different plasma regions. Therefore, in a statistical study the plasma parameters vary more smoothly along the orbit the Moon as in the situation where the upstream parameters are relatively unchanged during a long time period. Fig. 2 shows the histogram of plasma parameters at four ϕ angles. In the ϕ = 0^o case the Moon is in the solar wind and, therefore, this distribution shows the upstream parameters used in the simulation. The mean densities in the ϕ angle 0^o, 20^o, 40^o and 60^o was ~6.9 cm^{-3}, ~7.3 cm^{-3}, ~8.6 cm^{-3} and ~6.1 cm^{-3}, respectively. The increase of the density at ϕ=20^o and 40^o indicates that these positions are occasionally with the magnetosheath while at ϕ =60^o the position is often within a region where the density becomes smaller than in the solar wind density. Moreover, the shape of the distribution function is quite similar in ϕ =0^o, 20^o and 40^o cases. At the ϕ =60^o the distribution is "pushed" to lower densities and it becomes more peaked near the maximum density occurrence value. The solar wind velocity is relatively similar in all histograms. Moreover, the mean velocity values are also much similar at four positions: ~440 km/s (ϕ=0^o), ~440 km/s (ϕ=20^o), ~400 km/s (ϕ=40^o), and ~390 km/s (ϕ=60^o). Also the distribution of the total magnetic field is much alike in all four cases as well as their mean values: ~7.2 nT (ϕ=0^o), ~7.6 nT (ϕ=20^o), ~8.9 nT (ϕ=40^o), and ~7.3 nT (ϕ=60^o). Largest changes along the orbit can be seen in the plasma temperature which increases all the way from the solar wind into the deep inside the tail the mean temperatures being ~1.5×10^6 K (ϕ=0^o), ~2.4×10^6 K (ϕ=20^o), ~6.6×10^6 K (ϕ=40^o), and ~1.2×10^7 K (ϕ=60^o).

The mean properties of the bulk velocity and the magnetic field along the analysed orbit are studied in details in Fig. 3. Three velocity components show that the velocity components do not differ much from the upstream parameters. However, some anticipated small changes in the direction of the velocity can be seen on the XY-plane where the Earth has diverged the solar wind flow away from it, that is, to the +y direction on the dusk side (y>0) and to the -y direction on the dawn side (y<0) (see Figs. 3c and 3e).

A slightly more changes can be seen in the magnetic field, although at the first approximation the magnetic field within the orbit of the Moon can be assumed to be like in the solar wind. The average IMF z component is small (Fig. 3i) indicating that the magnetic field lines are on average near the ecliptic plane like they were in the solar wind. In Figs. 3g and 3h the mean B_x and B_y components are derived by calculating mean values -sign(B_y)×B_x and -sign(B_y)×B_y values, respectively. Note that by using the sign of the B_y component, we take into account the fact that part of the time the Earth was on the "toward" sector when the IMF is pointing toward the Sun and when B_x>0 and B_y< 0, and part of the time in the "away" sector when the IMF is pointing away the Sun and when B_x<0 and B_y>0. The -sign(B_y) mirrors the "away" IMF sector cases into the "toward" IMF sector but it does not average out the cone angle, or the Parker spiral angle, information. As can be seen in Fig. 3h) the Earth slightly changes the direction of the magnetic field from the nominal direction of the IMF within the tail so that the magnetic field orientation is there more along the Earth-Sun line that in the solar wind.

The statistical values of the analysed plasma and field values along the lunar orbit are shown in Fig. 4. In addition to the median value (i.e. the 50^{th} percentile, or the 2^{nd} quartile Q2) it shows the variations of the data by giving the 25^{th} percentile (i.e. the 1st quartile, Q1) which is the value below 25% of the values are, and the $75t^h$ percentile (i.e. the 3rd quartile, Q3) above which 25% or the values are. When the parameter changes are studied by moving from the position ϕ = 0^o to the position ϕ = 90^o the density can be seen first slightly to increase in the magnetosheath and then to decrease deeper in the tail (Fig. 3a). The plasma temperature can be seen to increase while moving toward the centre of the tail (Fig. 4d). The thermal pressure increases first in the magnetosheath,

decreases in the magnetic tail lobes but increases again near centre of the tail which is the point where the plasma sheet is anticipated to be located most frequently in the analysed positions (Fig. 4c). As already mentioned, the bulk velocity and the magnetic field changes are relatively small from position to position.

An important piece of information can be seen in Fig. 4 by looking how the 25th and 75th percentiles are located with respect to the median values and what is the difference between the 25th percentile and the 75th percentile because this indicates how the Earth has disturbed the initial distribution function of the macroscopic plasma parameters. When the relative fluctuations were analysed by calculating by defining a fluctuation ratio parameter f ≡ [(75th percentiles – 25th percentiles)/median] it was found f are quite similar for the density (f ~0.9-1.3), the bulk velocity (f ~0.25-0.5), thermal pressure (f ~0.5-1.2), temperature (f ~0.6-1.2) and the magnetic field (f ~0.6-0.8) values along the orbit (figures not shown). These relatively small changes of the fluctuation ratio suggests that the source of the fluctuations on the orbit of the Moon are mainly related to the fluctuations of the solar wind, that is, variations of these parameters in the Earth's tail reflect relatively passive variations of the solar wind.

The location of the positions where the Earth disturbs the solar wind plasma is illustrated in Fig. 5. In Fig. 5 mean values are plotted on the orbit so that the radial distance from the orbit is related linearly on the value of the parameter. At the centre of the tail the density of plasma is decreased, and the plasma is hot. The thermal pressure increases in the magnetosheath. Not much change can be seen in the bulk velocity or in the magnetic field.

The temperature of electrons, T_e, and the density of electrons, n_e, determine the length of the Debye length λ_D which is $\sim 69\sqrt{T_e[K]/n_e[cm^{-3}]}$ meters. If we assume that the plasma is quasi-neutral, the electron density is equal to the plasma density derived from the MHD model. As long as only the plasma density is considered, the decrease of the density seen in Fig. 4a would therefore result in the increase of the Debye length. A MHD model does not give information of how the electron density is related to the plasma temperature but if we assume, for simplicity, that the electron temperature is equal the plasma density obtained from the simulation, the Debye length is anticipated to increase deep in the tail also because of the increase of the temperature (c.f. Fig. 4d).

In Fig. 6 the change of the Debye length is analysed in more detail by assuming a quasi-neutrality and approximating that the electron temperature is equal the plasma density. Fig. 6 suggests a large spatial expansion of the Debye sheath when the Moon moves from the solar wind deep into the tail. In the solar wind the size of the Debye layer is order of meters. According to the PIC simulations that results a plasma layer above the surface which size is order of a ten meter (e.g. Poppe and Horànyi, 2010; Kallio et al 2014). Deep in the tail the size of the Debye layer can be of the order of a hundred meter. According to PIC simulations, such a situation will result in a highly extended plasma layer above the lunar surface (Poppe et al., 2011). Overall, Fig. 6 implies that the location of the Moon has to be taken into account when it is deep in the tail when the direct plasma-surface processes are studied.

4. Discussion

In this paper statistical parameters near the lunar orbit have been analysed in order to estimate how the Earth disturbs the solar wind plasma near the Moon. Plasma parameters are important because they affect various small and large scale physical processes near the surface and around the Moon. The plasma parameters were derived from a 3D magnetohydrodynamic GUMICS-4 simulation for the time period Jan 2002 – Feb 2003.

The advantage of the derived plasma parameter near the lunar orbit is that the dataset gives a possibility to study simultaneously plasma parameter in the undisturbed solar wind and in the disturbed region in the magnetosheath and in the magnetotail. In such a way the response of the magnetosheath and magnetospheric parameters to the upstream parameters can be studied. Furthermore, generally speaking, the one year run provides a possibility to

generate a large dataset for various upstream conditions. Such a dataset can only seldom be obtained from observations. For example, there were no spacecraft orbiting the Moon during the year 2002 which is analysed in this paper.

However, there are several important issues which have to be taken into account in the used simulation dataset. First of all, in a MHD simulation the derivation of the thermal pressure can cause problems because it is not a primary parameter in the model but it is derived afterwards from the total internal energy density by removing the energy density associated with the bulk velocity and the magnetic energy density. In fact, if one wants to keep exact conservation laws there is no guarantee that the obtained thermal pressure is always positive (see Janhunen, 2000). This is a potential source of inaccuracies when the Debye layer region is analysed and modelled because the size of the Debye layer and the surface potential depends on the electron temperature (see e.g. Nitter et al., 1998). Every model also has its own characteristic features which role to the solution should be taken into account. For example, magnetic tail lobes, the magnetotail, and the night side magnetopause has been found to be smaller in the GUMICS simulations at typical solar wind and interplanetary magnetic field (IMF) conditions than is measured by various spacecraft (Gordeev et al., 2013). In the future simulated plasma parameters in the far tail could be compared with the data obtained from the THEMIS/ARTEMIS mission (Angelopoulos, 2008, 2011) far tail measurements (Vörös et al., 2014).

The study presented in this paper leaves therefore room for further analysis where the derived plasma parameter are studied in more detail, for example, by studying in detail how the changes of the parameters are related to the exact position of the plasma boundaries. Furthermore, recently, in addition to measurements from ARTEMIS mission (e.g. Poppe et al., 2012) also plasma measurements near the Moon have become available from the KAGUYA (e.g. Yokota et al., 2009) and Chandrayaan-1 (e.g. Futaana et al., 2010) missions. Choosing events from the simulated data set where the upstream parameter was much alike during the *in situ* measurements near the Moon could help to study accuracy of the simulated plasma parameter. Moreover, making runs for the time intervals when *in situ* data is available would enable a detailed evaluation of the accuracy of the simulated data. More analysis is therefore called for to study in detail the properties of the ambient plasma near the Moon at different solar wind conditions.

Summary

Properties of plasma and the magnetic field relevant to analyse plasma physical processes around the Moon have been studied. Analysis of the simulated dataset based on a global MHD simulation suggests that the Earth does not disturb strongly the velocity and the magnetic field along the orbit of the Moon. The plasma density and the plasma temperature downstream of the bow shock are, instead, disturbed strongly by the Earth. These periodic variations along the orbit of the Moon affect also the size of the Debye length and, consequently, the near surface plasma processes. Overall, the derived statistical plasma parameters make it possible to analyse in detail the direct plasma-surface interaction at the Moon even when it is in the disturbed plasma regions.

References:

Angelopoulos, V., 2008, The THEMIS Mission. Space Science Reviews 141, 5–34.

Angelopoulos, V., 2011, The ARTEMIS Mission. Space Science Reviews 165, 3–25.

Facskó, G., Honkonen, I., Juusola, L., Viljanen, A., Tanskanen, E. I., Palin, L., Živković, T., Ågren, K., Opgenoorth, H., Vanhamäki, H., Janhunen, P., Palmroth, M., Kallio, E., Milan, S., 2014, Comparison of one year long gumics-4 global MHD simulation to spacecraft and ground based measurements, Journal of Geophysical Research. *in preparation*

Futaana, Y., S. Barabash, M. Wieser, M. Holmström, A. Bhardwaj, M. B. Dhanya, R. Sridharan, P. Wurz, A. Schaufelberger, and K. Asamura, 2010, Protons in the near-lunar wake observed by the Sub-keV Atom Reflection Analyzer on board Chandrayaan-1, J. Geophys. Res., 115, A10248, doi:10.1029/2010JA015264.

Gordeev, E., G. Facskó, V. Sergeev, I. Honkonen, M. Palmroth, P. Janhunen, and S. Milan, 2013, Verification of the GUMICS-4 global MHD code using empirical relationships, J. Geophys. Res. Space Physics, 118, 3138–3146, doi:10.1002/jgra.50359.

Holmström, M., Fatemi, S., Futaana,Y., Nilsson, H., 2012, The interaction between the Moon and the solar wind, Earth, Planets and Space, 64, 237–245, http://dx.doi.org/10.5047/eps.2011.06.040.

Janhunen, P., 2000, A positive conservative method for magnetohydrodynamics based on HLL and Roe methods, Journal of Computational Physics, 160, 649–661.

Janhunen, P., M. Palmroth, T. V. Laitinen, I. Honkonen, L. Juusola, G. Facskó, and T. I. Pulkkinen, 2012, The GUMICS-4 global MHD magnetosphere–ionosphere coupling simulation, J. Atmos. Sol. Terr. Phys., 80, 48–59, doi:10.1016/j.jastp.2012.03.006.

Jarvinen, R., Alho, M., Kallio, E., Wurz, P., Barabash, S., and Y. Futaana, 2014, On vertical electric fields at lunar magnetic anomalies, Geophys. Res. Lett., 41, 22432249, doi:10.1002/2014GL059788.

Kallio, E., 2005, Formation of the lunar wake in quasi-neutral hybrid model, Geophysical Research Letters, 32, L06107, http://dx.doi.org/10.1029/2004GL021989.

Kallio, E., R. Jarvinen, S. Dyadechkin, P. Wurz, S. Barabash, F. Alvarez, V. Fernandes, Y. Futaana, J. Heilimo, C. Lue, J. Makela, N. Porjo, W. Schmidt and T. Siili, 2012, Kinetic simulations of finite gyroradius effects in the lunar plasma environment on global, meso, and microscales, Planetary and Space Science, http://dx.doi.org/10.1016/j.pss.2012.09.012.

Kallio, E. et al., 2014, Dust environment of an airless object in kinetic models, Planetary and Space Physics. *submitted*

Mall, U., E. Kirsch, K. Cierpka, B. Wilken, A. Söding, F. Neubauer, G. Gloeckler, and A. Galvin, 1998, Direct observation of lunar pick-up ions near the Moon, Geophys. Res. Lett., 25(20), 3799–3802, doi:10.1029/1998GL900003.

Nitter, T., Havnes, O., Melandso, F., 1998, Levitation and dynamics of charged dust in the photoelectron sheath above surface in space, J. Geophys. Res., 103(A4), 6605–6620, http://dx.doi.org/10.1029/97JA03523.

Poppe, A., and M. Horànyi, 2010, Simulations of the photoelectron sheath and dust levitation on the lunar surface, J. Geophys. Res., 115, A08106, doi:10.1029/2010JA015286.

Poppe, A., J. S. Halekas, and M. Horányi, 2011, Negative potentials above the day-side lunar surface in the terrestrial plasma sheet: Evidence of nonmonotonic potentials, Geophys. Res. Lett., 38, L02103, doi:10.1029/2010GL046119.

Poppe, A. R., R. Samad, J. S. Halekas, M. Sarantos, G. T. Delory, W. M. Farrell, V. Angelopoulos, and J. P. McFadden, 2012, ARTEMIS observations of lunar pick-up ions in the terrestrial magnetotail lobes, Geophys. Res. Lett., 39, L17104, doi:10.1029/2012GL052909.

Sibeck, D. G., and R.-Q. Lin, 2014, Size and shape of the distant magnetotail, J. Geophys. Res., Space Physics, 119, 1028–1043, doi:10.1002/2013JA019471.

Vörös, Z., G. Facskó, M. Khodachenko, I. Honkonen, P. Janhunen, M. Palmroth, 2013, Windsock memory COnditioned RAM (CO-RAM) pressure effect: Forced reconnection in the Earth's magnetotail, J. Geophys. Res., DOI: 10.1002/2014JA019857.

Yokota, S., et al., 2009, First direct detection of ions originating from the Moon by MAP-PACE IMA onboard SELENE (KAGUYA), Geophys. Res. Lett., 36, L11201, doi:10.1029/2009GL038185.

Acknowledgements

The authors thank ECLAT, IMPEX and DEPM projects for the financial support for the study. The GUMICS-4 runs were made by the Finnish Meteorological Institute, Helsinki, Finland, in the ECLAT project funded by the European Union (the Grant Agreement No. 263325). The IMPEx (Integrated Medium for Planetary Exploration) project was funded by the European Union, the Grant Agreement No. 262863. The DPEM project is funded by European Space Agency (ESA ITT, AO-1-6696/11/NL/CO). The authors acknowledge the ECLAT and the IMPEx projects for the MHD simulations and for the access to the simulated data and the DPEM team for discussions of the Moon-solar wind interaction and dusty plasma.

Figure Caption

Fig. 1. An example of how the properties of plasma vary near the orbit of the Moon: (top left) Particle density, (top right) bulk velocity, (bottom left) plasma temperature and (bottom right) the magnitude of the magnetic field. The plasma and field values are derived from the year run made by GUMICS-4 model (Facskó et al., 2014, in preparation). Parameters correspond the situation on February 20, 2002 at 08:54 (UT). The values of the simulation was plotted on the GSE XY-plane (x_{GSE} = [30, −64] R_E, y_{GSE} = [−64, 64] R_E, z_{GSE} = 0 R_E). The dots are plotted on the positions (x_{GSE}, y_{GSE}, z_{GSE}) = ($60R_E \cos(90^o + \phi)$, $60R_E \sin(90^o + \phi)$, 0) where $\phi = 0^o, 1^o, .., 180^o$ and they show approximate position of the lunar orbit.

Fig. 2. Histograms of the density (top column), the bulk velocity (the 2nd column from the top) and the temperature (the 3rd column from the top) of the plasma and the total magnetic field (bottom column) at four positions near the lunar orbit: (a-d) $\phi=0^o$, (e-h) $\phi=20^o$, (i-l) $\phi=40^o$, and (m-p) $\phi=60^o$.

Fig. 3. The mean bulk velocity and the magnetic field near the lunar orbit. The angle in the panel e) shows the orientation of the flow on the ecliptic plane. The magnetic field B_x and B_y values are mean magnitudes and in such a way the Parker spiral IMF on the magnetic equator is projected on the "toward" IMF sector (see text for details). The cone angle in panel j), or the Parker spiral angle, is the angle between the magnetic field on the XY-plane and the x-axis.

Fig. 4. Statistical values of the plasma and magnetic field near the orbit of the Moon. The solid lines are median values, the dashed lines below the median lines are the 25 h percentiles and the dashed lines above the median values are the 75th percentiles.

Fig. 5. Mean plasma and field values near the Moon plotted on the lunar orbit. The radial distance of the black region above the point depends linearly on the value of the shown parameter. In the figures the Sun is on the left.

Fig. 6. The size of the Debye length near the orbit of the Moon in the case when the temperature of electron is assumed to be equal the temperature of plasma which is derived from the GUMICS-4 simulation. The values are median (the solid line), the 25th percentile (the lower dashed line) and the 75th percentile (the upper solid line).